Effect of Antenna Element Properties and Array Orientation on Performance of MIMO Systems

Arindam Pal, Beng Sin Lee, Phill Rogers, Geoff Hilton, Mark Beach and Andy Nix
Centre for Communications Research
University of Bristol
Bristol, UK
e-mail: A.Pal@bris.ac.uk

Abstract— **This paper presents a MIMO throughput based assessment of three candidate antenna arrays, each of which was constructed from a different type of antenna element. A model of the MIMO channel resolved in orthogonal polarization planes was employed to apply multipath parameters of the channel to antenna array patterns, in order to predict the antenna-gain inclusive channel response. Based on simulations of the antenna inclusive channel, an analysis of the effect of antenna element properties including directivity, efficiency and polarization on the statistics of the overall MIMO channel response is presented.**

Keywords- multiple-input multiple-output systems; propagation modelling, polarization, antenna properties

I. INTRODUCTION

The performance benefits of employing multiple antennas at both transmitting and receiving ends of a wireless link and the effect of physical parameters of the channel on performance have been widely reported [1],[2]. However, the problem of designing antennas and antenna arrays specifically for MIMO applications is as yet to be fully addressed. Antenna properties are usually either excluded or isotropic antenna patterns are assumed for modeling the MIMO wireless channel. In reality, the antenna gain has a significant effect on the statistics of the signal and the choice of antenna element is particularly important for systems where transmit power is limited. In this paper, we focus on peer-to-peer MIMO systems involving hand-held devices operating at 5.2 GHz. In order to investigate the effect of antenna properties on performance, three 4-element candidate array designs were constructed, each from a different type of antenna element. All three arrays were designed for a Personal Digital Assistant (PDA) application. The candidate elements were chosen because they differed widely in their efficiencies, polarization purities and directivities. The polarization purity of an antenna, i.e. the extent of linearity in polarization, can vary widely between antennas. Since the variation in cross-polar discrimination (XPD) in the wireless channel can also be significant [3], there is a need to investigate the effect of polarization purity on performance.

The model of the MIMO channel employed here includes the complete antenna characterization as it employs 3-D complex gain patterns resolved orthogonally in the polarization domain. The patterns are applied to multipath gains that are also derived in orthogonal polarization planes, in order to predict the antenna-inclusive MIMO channel response. Indoor peer-to-peer wideband channel measurements were conducted with pairs of identical sets of the candidate PDA arrays at opposite ends of the link [4]. The model has been validated through comparison with the channel measurements [5].

The paper begins by describing the design and construction of the candidate PDA arrays (Section II). The model of the polarized antenna-inclusive MIMO channel is described in Section III. Based on simulations of the 4×4 MIMO channel employing either the candidate PDA arrays or certain hypothetical arrays, an analysis of the various effects of antenna properties is presented in Section IV.

II. CANDIDATE ANTENNA ARRAYS

A. Antenna element types

Each of the three antenna arrays was constructed from four elements of the same type. The elements were placed to mount on the surface of a PDA-type case 63×113×14 mm. All the elements were designed to operate at 5.2 GHz, with a -10 dB input bandwidth in excess of 120 MHz. A brief description of the elements is as follows:

- The Linear Slot (Slot) antenna element was a cavity-backed stripline-fed antenna. The antenna was fabricated using 1.6 mm thick Rogers RT/duroid 5880 and measured 40×14×3.2 mm. Four slots were flush-mounted on a suitable diecast box.
- The Dielectric Resonator Antenna (DRA) based design employed a ceramic puck measuring 11×4.8×3.2 mm mounted on a small pcb assembly of 50×10 mm. Four single elements were soldered to a PDA sized copper box to simulate the PDA device.
- The Planar Inverted-F Antennas (PIFA) was fabricated on 0.8 mm Taconic TLY5 with a dielectric constant of 2.2. The radiating surface covered 13.5×3.5 mm beyond the ground plane and 4 such elements were mounted approximately 21 mm apart within the PDA.

The element patterns and their placements within each array are shown in [4]. Since all elements are directive, they were placed and oriented in each case so as to achieve large overall directional coverage.

B. Antenna Gain Patterns

The far-field 3-D radiation patterns of the three antenna arrays at 5.2 GHz were obtained through measurements in an anechoic chamber. In the far-field region of an antenna, the plane wave assumption holds true and the measured radiation can be split into orthogonal components. The complex E-field gain in orthogonal components of polarization (E_θ, $E_\emptyset$) was recorded for all directions (θ, $\emptyset$) in the 3-D space (see Figure 6). The power gain of an antenna in any direction is given by the product of efficiency and directive gain of the antenna [6]. Thus, the antenna gain (G_θ, $G_\emptyset$) was derived from the measured E-fields for arbitrary efficiencies. The complex element pattern gains contained the relative phase differences between the elements for each direction-of-radiation incident on the array. This eliminated the need to model separately the locations or orientations of the elements within the arrays. The average directivities, radiation efficiencies, and co-polar powers as derived from the pattern measurements are shown in TABLE I. Co-polar power is the percentage of radiated power that can be resolved to a single polarization plane.

TABLE I. ANTENNA ELEMENT PROPERTIES

Antenna Type	*Directivity*	*Efficiency*	*Co-polar Power*
Slot	7.1 dB	81 ± 3.7%	94%
DRA	4.7 dB	39 ± 2.7%	81%
PIFA	6.9 dB	60 ± 10.0%	59%

It can be seen that the Slot antenna offers the highest efficiency and directivity as well as greatest polarization purity. The DRA offers moderate polarization purity, but has a lower efficiency. The PIFA has slightly better efficiency, but almost no cross-polar discrimination.

III. MODELLING THE POLARISED MIMO CHANNEL

A. Ray-based propagation model

The propagation characteristic of an open-plan office of dimensions 12×18 m was simulated using the ray-launching algorithm [7]. The reflection coefficients of the scatterers were modeled for the vertical and horizontal polarization planes. The multipath rays that were extracted for each link were described by their direction-of-arrival (DOA), direction-of-departure (DOD), excess delay, gain and phase. Both azimuth and elevation angles were obtained for the DODs and the DOAs. The multipath components (MPCs) for each link were derived for both vertically and horizontally polarized isotropic antennas placed at both the transmitter and the receiver. Thus, multipath gains were obtained for four combinations of Tx-Rx polarizations: vertical-vertical (h^{vv}), vertical-horizontal (h^{vh}), horizontal-vertical (h^{hv}) and horizontal-horizontal (h^{hh}).

The channel was simulated for a fixed transmitter placed at a central location in the room, and for receivers placed at about 4000 evenly spaced points throughout the grid. The heights of the transmitter and the receiver were chosen to be 1.3 m and 0.8 m respectively. The XPD of the channels obtained from the model varied from -5 dB to 14 dB, with a mean of 1.9 dB. We define the XPD at each location snapshot as the ratio between the total powers of the horizontal and the vertical MPCs. The RMS delay spreads were in the range of 5-10 ns.

B. Calculating MIMO response

The multipath gains that were obtained from the deterministic model were resolved in horizontal and vertical directions. However, the orthogonal components of measured gain patterns (G_θ, $G_\emptyset$) did not correspond to vertical and horizontal planes of polarization. Therefore, the gain patterns were re-resolved to horizontal and vertical components G_h and G_v respectively, using the technique described in [5].

The multipath rays were assumed to impinge upon the antennas as plane waves. The channel response was derived from the product of antenna pattern gains and multipath gains using (1). All the MPCs that were extracted for each location snapshot were assigned to the nearest delay tap. The response at each tap in each polarization plane (horizontal or vertical) was calculated from the summation of the overall 'gains' of all rays arriving at the receiver in that plane. Care had to be taken to match the components of polarization at each antenna-channel interface. For instance, the multipath gain h^{vh} was multiplied by the vertical gain component at the transmitter and horizontal gain component at the receiver.

$$H_{j,k,\ell} = \sum_{s=1}^{n_\ell} \begin{bmatrix} G_v^{Tx_j}(\Psi_s) \\ G_h^{Tx_j}(\Psi_s) \end{bmatrix}^T \begin{bmatrix} h_s^{vv} & h_s^{vh} \\ h_s^{hv} & h_s^{hh} \end{bmatrix} \begin{bmatrix} G_v^{Rx_k}(\Omega_s) \\ G_h^{Rx_k}(\Omega_s) \end{bmatrix} \quad (1)$$

In (1), $H_{j,k,\ell}$ is the channel response from transmit element j to receive element k at the ℓth delay tap. n_ℓ is the number of rays at each delay-tap ℓ, Ψ_s and Ω_s are the DOD and DOA of the sth ray in the ℓth tap. The subscript ℓ has been omitted from $\Psi_{\ell,s}$, $\Omega_{\ell,s}$ and $h_{\ell,s}$ in the remaining part of equation for clarity.

C. Calculation of capacity

The capacity that is calculated after normalizing the channel response to average received power of unity indicates the level of correlation between elements of the channel matrix, and shall be referred to as gain-normalized capacity (C_g). However, since an evaluation of antennas is being made, it is preferable to preserve the relative received powers of all the links in the calculation of capacity (for fixed transmit power). This is achieved by compensating the channel response for only the estimated pathloss between the locations of the transmitter and the receiver, which gives the pathloss-normalized capacity (C_p). Pathloss normalization was achieved by dividing the channel response by the overall pathgain (inverse of pathloss), as shown in (2). The overall pathgain is given by the summation of pathgains for each polarization plane at the transmitter, weighted by the ratio of power transmitted by the array in that plane.

$$H_{j,k,\ell}^{norm} = \frac{H_{j,k,\ell} \cdot \sqrt{n_F}}{\sqrt{r_h \sum_{s=1}^{n_S} \left(\left|h_s^{hv}\right|^2 + \left|h_s^{hh}\right|^2 \right) + r_v \sum_{s=1}^{n_S} \left(\left|h_s^{vh}\right|^2 + \left|h_s^{vv}\right|^2 \right)}} \quad (2)$$

In (2), n_S is the total number of multipath rays at each link, n_F is the number of taps, and r_h and r_v are the ratios of power transmitted in the horizontal and vertical polarizations respectively. Note that ($r_h = 1 - r_v$). The above normalization also compensates for the effect of non-unity average XPD of the channel, which is needed as the candidate arrays radiate different amounts of power in horizontal and vertical polarization planes. The normalised capacity of the frequency selective channel was calculated from the normalized channel response using the well known equation given in [1].

IV. Analysis of Results

A. Model Simulations

In order to observe the effect of each antenna property on the MIMO channel, the model described in Section III was applied for the following conditions.

1) The MIMO channel response was derived for identical arrays placed at both ends of the link. The results presented in Sections IV.B and IV.C are derived for fixed and identical orientations of transmit and receive arrays over many locations of the Rx array. Section IV.D presents the effect of orientation for a fixed location of the Tx and Rx arrays.

2) Efficiency: It can be seen from (1) that the total received power of each MIMO link varies linearly with the product of efficiencies of transmit and receive elements. Since identical arrays are being used at both Tx and Rx ends, there is a 2 dB change in the total received power for every 1 dB change in efficiency of the elements. In order to demonstrate the effects of the antenna properties other than efficiency, all the presented results have been derived for 100% efficiency of the antenna elements.

3) Hypothetical arrays: The candidate PDA elements have different beam patterns, directivities, polarization purities, placements and orientations, all of which have an effect on the properties of the MIMO channel response. In order to observe the effect of only polarization, three hypothetical 4-element arrays were considered in addition to the candidate PDA arrays. The three arrays were – the Co-Polarized (COP) array, the Cross-Polarized (CRP) array, and the Un-Polarized (UP) array. The constituent elements of these arrays were assigned isotropic gain patterns, 100% efficiency, and polarization properties as given in TABLE II.

TABLE II. Element Gains of Hypothetical Arrays

Antenna Array	Isotropic Power Gain in Vertical (V) and Horizontal (H) Polarizations, shown as (V, H).			
	Element #1	***Element #2***	***Element #3***	***Element #4***
COP	(1, 0)	(1, 0)	(1, 0)	(1, 0)
CRP	(1, 0)	(0, 1)	(1, 0)	(0, 1)
UP	(0.5, 0.5)	(0.5, 0.5)	(0.5, 0.5)	(0.5, 0.5)

Since the phase patterns of the three PDA arrays were found to be uncorrelated, the above theoretical arrays were also assigned independent phase patterns. It may be noted that the construction of the Slot and the DRA arrays is similar to that of the CRP array, with two linear elements radiating predominantly in the vertical plane and two in the horizontal. The UP array is an exaggerated version of the PIFA array, as its elements have no cross-polar discrimination in any direction-of-incidence.

B. Received Power

The cumulative distributions of the average received power for the Hypothetical and PDA 4×4 MIMO links are shown in Figure 1. Since received power is related to antenna gain, elements with larger directivities could be expected to experience greater variation in received power. Hence, the PDA arrays show greater variation in received power than the Hypothetical arrays, which have element directivities of 0 dBi.

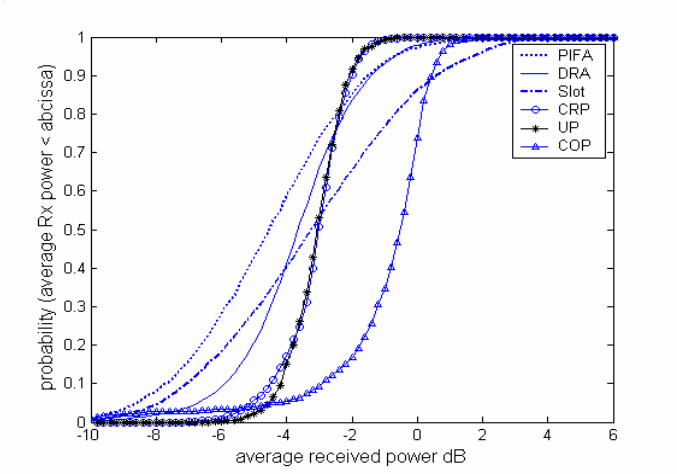

Figure 1. cumulative distribution functions (cdfs) of the received powers of the PDA and Hypothetical links averaged in each case over 16 subchannels. Derived for 100% efficiency of elements and 0 dB pathloss in the channel.

Average received power is maximized when both transmit and receive arrays are constructed from identically oriented linearly polarized elements (COP). The CRP arrays on average received half (-3 dB) of the total transmitted power (for unity pathloss) because the constituent subchannel links are equally likely to be either perfectly matched or mismatched in polarization. The UP arrays also receive lower power than the COP link, as there are losses at the receiver due to the splitting of signal power in the polarization domain. The CRP and UP links receive very similar total powers, but the distribution of power amongst the constituent subchannels is different, as shown in Figure 2.

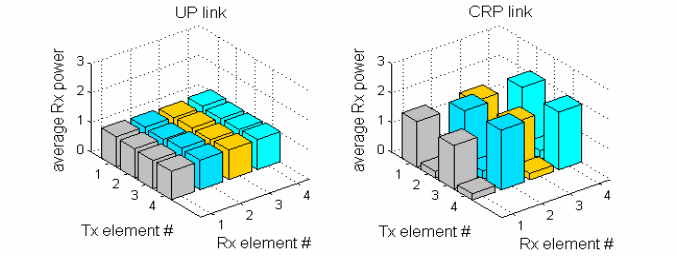

Figure 2. Average received power in (4x4 = 16) constituent subchannels of the UP and CRP MIMO links, for all locations of Rx array on the grid

C. Channel Correlation and Capacity

Correlation between MIMO subchannels is dependent on properties of the channel (e.g. richness of scattering, angular spread [2]) as well as the antenna elements (e.g. mutual coupling, spacing, orientation [8]). Spatial correlation varies inversely with gain-normalized capacity (C_g). The C_g of all the links is shown in Figure 3.

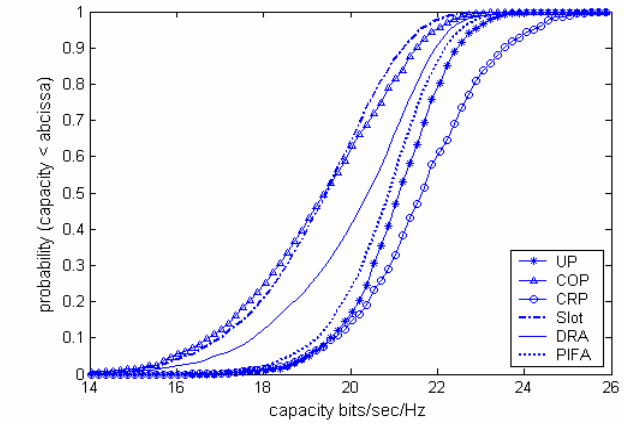

Figure 3. cdfs of gain-normalized capacity of the 4x4 PDA and Hypothetical links, derived for all locations of Rx array on the grid

The CRP and the UP links offer significantly better de-correlation than the COP arrays as they exploit the diversity offered by the polarization domain. The PDA arrays exploit to different extents the diversity offered by the polarization and directional domains through diverse orientations of polarized and directive elements respectively. Since the Hypothetical arrays were assigned independent phase patterns, they achieve better C_g than their corresponding PDA links. For example, the Slot arrays achieve a C_g much lower than that of the CRP arrays. In contrast, the PIFA arrays offer only marginally lower C_g than the UP arrays, which could be attributed to the de-correlation caused by mutual coupling as the PIFA elements were closely spaced [8]. The above observations indicate that in reality, un-polarized elements (e.g. PIFA) are likely to be more de-correlated than linearly polarized elements (e.g. Slot). The combined effect of channel correlation and received power on performance can be seen from the pathloss-normalized capacities, as shown in Figure 4.

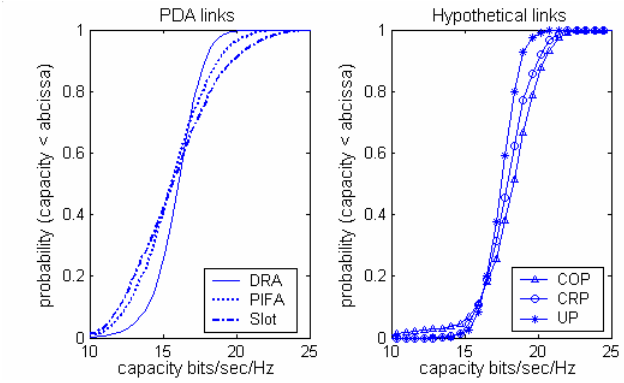

Figure 4. cdfs of pathloss-normalized capacity of the 4x4 PDA and Hypothetical links, derived for all locations of Rx array on the grid

D. Effect of array orientation on performance

The results presented in sections III.B and III.C are for fixed and identical orientations of transmit and receive arrays. In reality, the orientation of hand-held devices such as PDAs is unlikely to be fixed. The variation in performance as the orientation of the Tx and Rx arrays is varied independently is shown in Figure 5. The chosen link (for Figure 5) had an estimated K-factor of -2.5 dB, pathloss of -53 dB and experienced rich directional scattering (108 rays). The orientations of the arrays were varied using the technique described in Appendix A. Patterns were derived for 40 different random orientations of the arrays in the 3-D space, and the channel was simulated for (40×40=1600) combinations of Tx and Rx orientations.

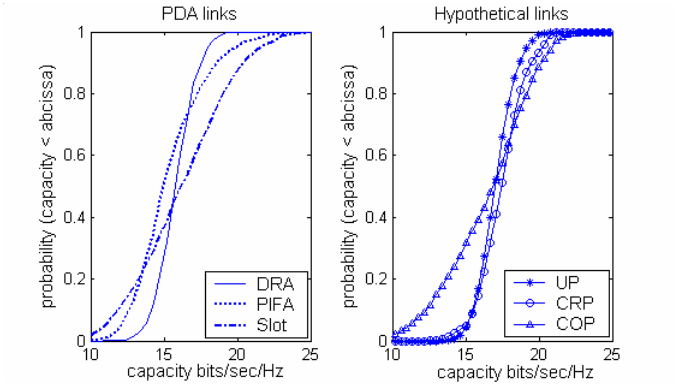

Figure 5. cdfs of pathloss-normalized capacity of the 4x4 PDA and Hypothetical links, derived for a large number of random orietations of the Tx and Rx arrays. Locations of Tx and Rx arrays are fixed.

The 10% outage capacity of the COP link is relatively low because the received power drops sharply as the transmit and receive arrays become mismatched in polarization. The UP and CRP links are more resilient to changes in orientation of the arrays. The CRP and UP arrays could also be expected to be more resilient to the level of XPD and cross-polar coupling in the channel, as they radiate equal powers in both orthogonal components of polarization. Thus, either cross-polarized linear elements (Slot) or unpolarized elements (PIFA) might be preferred for deployment in portable MIMO devices, depending on the element efficiencies (see TABLE I.) and the signaling scheme being employed (see Figure 2). It can be seen from Figure 4 and Figure 5 that lower element directivities generally give rise to smaller variation in performance and hence better outage capacities (note that the DRA elements are least directive).

CONCLUSIONS

Unpolarized elements offer good de-correlation and lower but more stable received powers. Linearly polarized elements offer the best received powers when the elements at both ends of the link are co-oriented. However, better de-correlation and resilience to orientation could be achieved through cross-polar placement of such elements, as needed for mobile hand-held devices such as PDAs. In general, superior outage capacities could be achieved through large coverage in both directional and polarization domains.

APPENDIX A.

Any rotation can be given as a composition of rotations about three axes and can be represented by a 3x3 rotation matrix **R**, which is essentially an orthogonal matrix [10]. The gain of the rotated antenna in direction $\mathbf{s} = [x_R \quad y_R \quad z_R]^T$ becomes equal to the value of pattern sampled originally at $\mathbf{r} = [x \quad y \quad z]^T$, where **s** is given by (3).

$$\mathbf{s} = \mathbf{R}\mathbf{r} \tag{3}$$

After rotation by **R**, the direction-of-incidence is rotated from (θ,ϕ) to (θ_R,ϕ_R), as given by (4) and (5).

$$\theta_R = \tan^{-1}\left(\frac{\sqrt{{x_R}^2 + {y_R}^2}}{z_R}\right) \tag{4}$$

$$\phi_R = \tan^{-1}\left(\frac{y_R}{x_R}\right) \tag{5}$$

The polarization components of the original gain pattern $F_\phi(\theta,\phi)$ and $F_\theta(\theta,\phi)$ represent the gains along directions $\hat{\mathbf{u}}_\phi$ and $\hat{\mathbf{u}}_\theta$ respectively. $\hat{\mathbf{u}}_\phi$ and $\hat{\mathbf{u}}_\theta$ are orthogonal to direction-of-incidence **r** and are given by (6) and (7).

$$\hat{\mathbf{u}}_\phi = [-\sin\phi \quad \cos\phi \quad 0]^T \tag{6}$$

$$\hat{\mathbf{u}}_\theta = [\cos\theta\cos\phi \quad \cos\theta\sin\phi \quad -\sin\theta]^T \tag{7}$$

The gain components of the rotated pattern in direction (θ_R,ϕ_R) could be resolved as $F_\phi(\theta,\phi)$ and $F_\theta(\theta,\phi)$. However, $F_\phi(\theta,\phi)$ and $F_\theta(\theta,\phi)$ would be the gains along the directions $\hat{\mathbf{v}}_\phi$ and $\hat{\mathbf{v}}_\theta$ respectively, where $\hat{\mathbf{v}}_\phi = \mathbf{R}\hat{\mathbf{u}}_\phi$ and $\hat{\mathbf{v}}_\theta = \mathbf{R}\hat{\mathbf{u}}_\theta$. Directional vectors $\hat{\mathbf{v}}_\phi$ and $\hat{\mathbf{v}}_\theta$ are orthogonal to **s,** but are not aligned with the directions of polarizations ($\hat{\mathbf{u}}_{\phi R}$, $\hat{\mathbf{u}}_{\theta R}$) that correspond to the new direction-of-incidence (θ_R,ϕ_R), as shown in Figure 6. $\hat{\mathbf{u}}_{\phi R}$ and $\hat{\mathbf{u}}_{\theta R}$ are defined in a similar way as $\hat{\mathbf{u}}_\phi$ and $\hat{\mathbf{u}}_\theta$, i.e. by replacing θ and ϕ with θ_R and ϕ_R respectively throughout the equations (6) and (7). The vectors ($\hat{\mathbf{v}}_\phi$, $\hat{\mathbf{v}}_\theta$) and ($\hat{\mathbf{u}}_{\phi R}$, $\hat{\mathbf{u}}_{\theta R}$) all lie in the same plane and the two sets are out of alignment by angle δ, as given by (8). As each direction-of-incidence is rotated from (θ,ϕ) to (θ_R,ϕ_R) due to rotation matrix **R**, the polarization components of the rotated gain pattern along directions $\hat{\mathbf{u}}_{\phi R}$ and $\hat{\mathbf{u}}_{\theta R}$ are given by (9).

$$\delta = \cos^{-1}\left(\hat{\mathbf{u}}_{\theta R}\cdot\hat{\mathbf{v}}_\theta\right) = \cos^{-1}\left(\hat{\mathbf{u}}_{\phi R}\cdot\hat{\mathbf{v}}_\phi\right) \tag{8}$$

$$\begin{bmatrix} G_{\theta R}(\theta_R,\phi_R) \\ G_{\phi R}(\theta_R,\phi_R) \end{bmatrix} = \begin{bmatrix} \cos\delta & \sin\delta \\ -\sin\delta & \cos\delta \end{bmatrix} \begin{bmatrix} F_\theta(\theta,\phi) \\ F_\phi(\theta,\phi) \end{bmatrix} \tag{9}$$

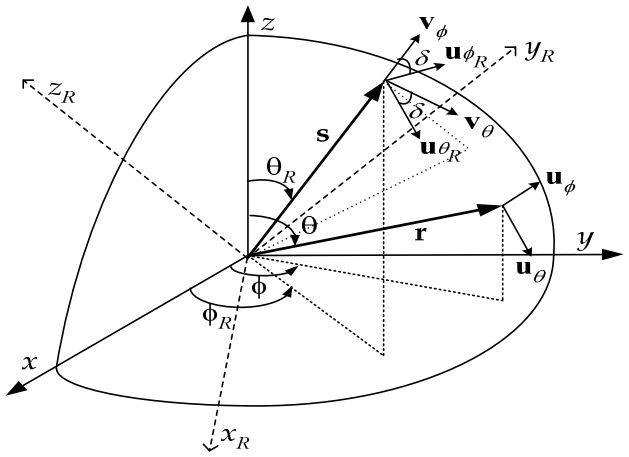

Figure 6. Directions of polarizations of element gain patterns before and after rotation.

ACKNOWLEDGMENT

The authors would like to thank the University of York and Antenova for providing the PIFA and DRA PDA arrays, and Ofcom for the support of the measurement campaign described in [4]. Arindam Pal would like to thank the UK ORS scheme and the University of Bristol for his postgraduate scholarship.

REFERENCES

[1] G. J. Foschini and M. J. Gans, "On Limits of Wireless Communications in a Fading Environment when Using Multiple Antennas", *Wireless Personal Communications*, pp. 311-355, 1998.

[2] D-S. Shiu, G. J. Foschini, M. J. Gans, and J. M. Kahn, "Fading Correlation and its effect on the Capacity of Multi-Element Antenna Systems", *IEEE International conference on Universal personal communications* (ICUPC'98), vol. 1, pp. 429–433, October 1998.

[3] P. Soma, D. S. Baum, V. Erceg, R. Krishnamoorthy, and A. J. Paulraj, "Analysis and modeling of Multiple-Input Multiple-Output radio channels based on outdoor measurements conducted at 2.5 GHz for fixed BWA applications", *ICC'02*, New York City, 2002.

[4] M. A. Beach, M. Hunukumbure, C. Williams, G. S. Hilton, P. Urwin-Wright, M. Capstick, and B. Kemp, "An experimental evaluation of three candidate MIMO array designs for PDA devices", *COST 273/284 Workshop*, June 2004.

[5] A. Pal, C. M. Tan, B. S. Lee, P. Rogers, G. Hilton, M. A. Beach and A. R. Nix, "Evaluation of Candidate MIMO Array Designs from Modelling and Measurements", *WPMC' 04*, Italy, September 2004.

[6] C. A. Balanis, *Antenna Theory, Analysis and Design*, Harper & Row Publishers Inc, New York, 1982.

[7] B. S. Lee, C. M. Tan, S. E. Foo, A. R. Nix and J. P. McGeehan, "Site Specific Prediction and Measurement of Indoor Power Delay and Power Azimuth Spectra at 5 GHz", *VTC 2001 Fall*. IEEE VTS 54th, vol. 2, pp. 733–737, 2001.

[8] M. K. Özdemir, E. Arvas, H. Arslan, "Dynamics of Spatial Correlation and Implications on MIMO Systems", *IEEE Communications Magazine,* no. 6, June 2004

[9] K. Tsunekawa and K. Kagoshima, "Analysis of a Correlation Coefficient of Built-in Diversity Antennas for a Portable Telephone," Proc. IEEE AP-S Int'l. Symp., vol. 1, pp. 543-46, Dallas, May 1990.

[10] E. W. Weisstein, "Rotation Matrix.", *MathWorld* - A Wolfram Web Resource, http://mathworld.wolfram.com/RotationMatrix.html, accessed in 2004.